Discovery and optimization of rapid manganese catalysts for the epoxidation of terminal olefins

Andrew Murphy, T. Daniel P. Stack *

Department of Chemistry, Stanford University, Stanford, CA 94305, USA

Available online 3 April 2006

Abstract

Twenty-two Mn^{II} complexes were screened for the catalytic epoxidation of terminal olefins using peracetic acid as the oxidant. A limited number of these complexes are efficient catalysts using peracetic acid solutions generated with H_2SO_4 (PAA_C), but most complexes are effective at 1 mol% catalyst loading using peracetic acid generated with strongly acidic resins (PAA_R). Under the less acidic conditions of PAA_R, $[Mn^{II}(phen)_2(CF_3SO_3)_2]$ has the highest activity of the catalysts screened, and epoxides terminal olefins using as little as 0.02 mol% catalyst within 5 min. The dimeric species $[Mn^{III,IV}_2(phen)_4(O)_2](ClO_4)_3$ is also a viable epoxidation catalyst with PAA_R, but the dimeric species is reduced by the residual H_2O_2 to monomeric Mn^{II} species under the reaction conditions. By comparison, a similar dimeric complex $[Mn^{III,IV}_2(R,R\text{-mcp})_2(O)_2](ClO_4)_3$, is not reduced by H_2O_2 under the reaction conditions and is not catalytically active, supportive of the notion that the catalytically relevant species is monomeric.
© 2006 Elsevier B.V. All rights reserved.

Keywords: Epoxidation; Manganese; Peracetic acid; Terminal olefins

1. Introduction

Metal-catalyzed oxygenations of organic substrates represent a widely used and studied class of reactions [1]. An important goal for developing new catalytic reactions is to discover catalytic epoxidation agents that are rapid, selective, inexpensive and flexible with respect to their substrate scope. Terminal olefins are a particularly challenging class of substrate to epoxidize due to their relatively electron-deficient nature [2–9], yet the resulting 1,2-epoxides are versatile starting materials for the synthesis of more complicated molecules [10]. Few simple catalytic systems for terminal olefin epoxidation exist that provide rapid conversion with high selectivity.

Uncatalyzed epoxidation of alkenes with peracids is a fundamental reaction in organic chemistry. Many terminal alkenes are susceptible to peracetic acid, but these epoxidation reactions require extended reaction times at elevated temperatures that often lead to reduced selectivity [11]. Combining transition metal catalysts with peracetic acid can enhance the epoxidation selectivity and reduce reaction times, as evidenced by the

good yields and high turnover frequencies of $[(Fe^{III}(phen)_2)_2(\mu\text{-O})(H_2O)_2](ClO_4)_4$ and Mn^{III} porphyrins at ambient temperatures [3,12]. Yet, in order for the highest reactivity to be attained, attention to the reaction medium acidity is often required. In the case of $[(Fe^{III}(phen)_2)_2(\mu\text{-O})(H_2O)_2](ClO_4)_4$, the optimal activity occurs at low pH presumably to allow facile peracid exchange at the iron center(s) [3], and the conversion of Mn^{III}(peracyl)porphyrin complexes to high-valent Mn-oxo(porphyrin) species is dependent strongly on the pK_a of the parent carboxylic acid of the peracid [13,14].

Only a few non-heme monomeric Mn^{II} complexes are known to be efficient epoxidation catalysts with H_2O_2 [15–17], and little is known about the oxidative reactivity of these catalysts with peracids. Our initial efforts in developing terminal olefin epoxidation catalysts focused on monomeric non-heme Mn^{II} complexes with commercial peracetic acid (PAA_C, 1% by wt. H_2SO_4) or a less acidic variant prepared with a strong acid resin (PAA_R) [18,19]. In contrast to $[(Fe^{III}(phen)_2)_2(\mu\text{-O})(H_2O)_2](ClO_4)_4$, which prefers strongly acidic conditions, only a limited number of Mn^{II} complexes are efficient catalysts with PAA_C. Fortunately, many are efficient catalysts with PAA_R at 1 mol% loading. Our efforts have focused on three such complexes $[Mn^{II}(R,R\text{-mcp})(CF_3SO_3)_2]$ (**1**), $[Mn^{II}(phen)_2(CF_3SO_3)_2]$ (**2**), and $[Mn^{II}(bpy)_2(CF_3SO_3)_2]$

* Corresponding author. Tel.: +1 650 725 8736; fax: +1 650 725 0259.
E-mail address: stack@stanford.edu (T.D.P. Stack).

(**3**). All three complexes exhibit exceptional turnover frequencies in terminal olefin epoxidation with peracetic acid under ambient conditions and are accessible from simple starting materials.

2. Results

2.1. Screening of Mn^{II}-complexes

Screening of the manganese complexes (Fig. 1), prepared in situ by mixing appropriate amounts of $Mn^{II}(CF_3SO_3)_2$ and ligand (L), initially focused on the epoxidation of 1-octene at 1 mol% loading for 5 min at room temperature (RT) with PAA_C [20,21]. Most complexes are poor catalysts under these conditions (Table 1) presumably due to their decomposition by ligand protonation. Indeed, $Mn^{II}SO_4$ often precipitates in the reactions, and such simple Mn^{II} salts are ineffective catalysts for terminal olefin epoxidation with peracetic acid. Only $[Mn^{II}(R,R\text{-mcp})(CF_3SO_3)_2]$, $[Mn^{II}(bisp)(CF_3SO_3)_2]$, and $[Mn^{II}(Me_3\text{-tacn})(CF_3SO_3)_2]$ (Table 1, entries 1, 9, 14) show significant catalytic activity.

With the less acidic PAA_R [18], 16 of the 22 complexes provide greater than 80% conversion with greater than 80% selectivity for 1,2-epoxyoctane at 1 mol% (Table 1) [22]. A

differentiation among these complexes is possible at 0.1 mol% catalyst loading, because only six complexes maintain high yields of 1,2-epoxyoctane: $[Mn^{II}(R,R\text{-mcp})(CF_3SO_3)_2]$ (**1**), $[Mn^{II}(phen)_2(CF_3SO_3)_2]$ (**2**), $[Mn^{II}(bpy)_2(CF_3SO_3)_2]$ (**3**), $[Mn^{II}(5\text{-Cl-phen})_2(CF_3SO_3)_2]$ (**4**), $[Mn^{II}(Me_3\text{tacn})(CF_3SO_3)_2]$, and $[Mn^{II}(bpma)(CF_3SO_3)_2]$. The first four complexes demonstrated the highest turnover frequencies ($>30 \, s^{-1}$) with excellent selectivity, which motivated further development.

2.2. Reaction conditions optimization

The stability of $[Mn^{II}(R,R\text{-mcp})(CF_3SO_3)_2]$ (**1**) under the acidic conditions created by PAA_C allows for efficient epoxidation of 1-octene at 0.1 mol% loading in CH_3CN with a turnover frequency of ca. $4 \, s^{-1}$. With PAA_R as the oxidant, the epoxidation reaction is nearly five-fold faster, and catalyst loadings as low as 0.02 mol% suffice to give good product yields. CH_3CN is the best solvent found for epoxidation with **1** and PAA_R or PAA_C; glacial acetic acid leads to lower product selectivity through appreciable epoxide ring-opening with acetate to form the 1,2-hydroxy-acetate products.

In contrast to **1**, **2**–**4** are only effective epoxidation catalysts of 1-octene at 0.1 mol% loading with PAA_R (Table 1) [19,23]. In CH_3CN, reducing the catalyst loading of **2** or **3**
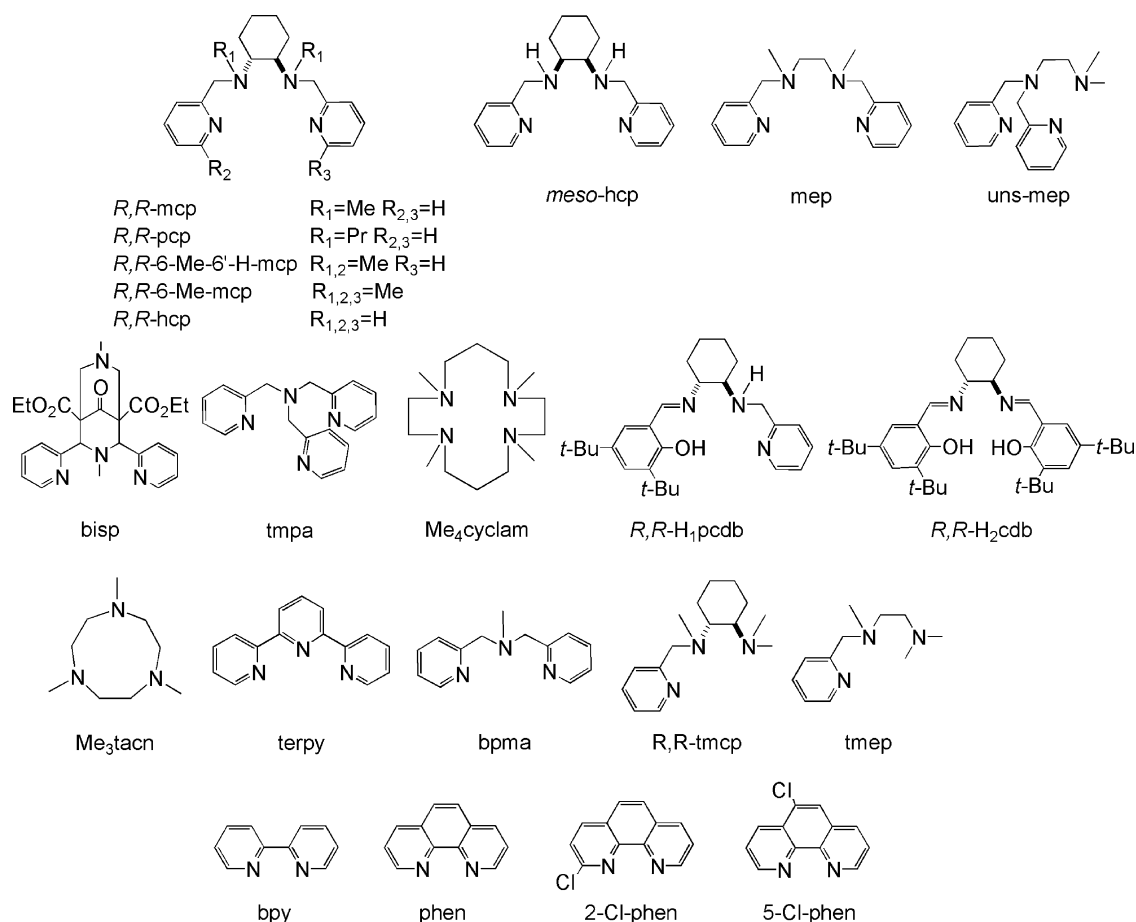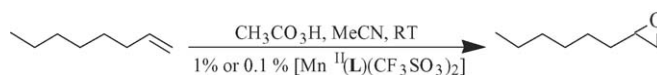

Fig. 1. Ligands used in this study.

Table 1
Epoxidation reactivity of [$Mn^{II}L(CF_3SO_3)_2$] complexes[a]

No.	Ligand	5 min		5 min				15 s[b]	
		PAA_C[c] oxidant		PAA_R[d] oxidant				PAA_R[d] oxidant	
		1% Catalyst loading		1% Catalyst loading		0.1% Catalyst loading		1% Catalyst loading	0.1% Catalyst loading
		Conv.	Epoxide	Conv.	Epoxide	Conv.	Epoxide	Epoxide	Epoxide
1	R,R-mcp	98	94	96	92	96	92	75	27
2	R,R-pcp	0	0	28	22	2	2	8	
3	R,R-6-Me-6′-H-mcp	18	15	91	88	36	31	19	
4	R,R-6-Me-mcp	6	2	60	55	6	4	10	
5	R,R-hcp	18	11	98	96	33	28	88	
6	meso-hcp	4	2	95	92	15	12	61	
7	mep	25	24	87	87	53	49	83	2
8	uns-mep	5	3	94	94	49	43	89	
9	bisp	97	91	92	84	23	18	19	
10	tmpa	3	2	96	92	6	4	23	
11	Me4cyclam	5	2	11	11	1	1	1	
12	R,R-H1pcdb[e]	6	6	51	49	6	5	50	
13	R,R-H2cdb[e]	4	2	20	15	1	1	3	
14	Me3tacn	80	71	95	91	85	82	44	8
15	terpy	2	1	94	91	50	46	84	43
16	bpma	0	0	88	83	82	77	83	2
17	R,R-tmcp	12	9	95	92	15	11	74	
18	tmep	1	1	88	86	10	9	57	
19	bpy[f]	2	2	99	95	99	94	94	93
20	phen[f]	2	2	99	93	99	93	93	93
21	2-Cl-phen[f]	1	1	46	40	7	3	7	
22	5-Cl-phen[f]	1	1	98	95	95	89	90	88
23	none	0	0	4	2	4	2	0	0

[a] 1-Octene (0.5 M) [$Mn^{II}L(CF_3SO_3)_2$] (5 mM), n-nonane (50 mM), 2 equiv. CH_3CO_3H, 25 °C, 5 min. Conversion and epoxide yields determined relative to an internal standard. Results are an average of at least three runs.

[b] 1-Octene (0.5 M) [$Mn^{II}L(CF_3SO_3)_2$] (5 mM), n-nonane (50 mM), 2 equiv. CH_3CO_3H (PAA_R), 25 °C. Reactions were quenched with Et_3N after 15 s.

[c] PAA_C: 32% CH_3CO_3H, 1% H_2SO_4 in CH_3CO_2H/H_2O.

[d] PAA_R: 9–10% CH_3CO_3H in CH_3CO_2H.

[e] [$Mn^{III}LOAc$] complexes were generated from $Mn^{II}OAc_2 \cdot 4H_2O$, L, and O_2.

[f] 2 equiv. of L/Mn^{II}.

to 0.02 mol% leads to lesser substrate conversion; the reaction terminates within 5 min with only ~65% conversion of 1-octene. Glacial acetic acid as the solvent enhances the epoxide yields using **2** as a catalyst with complete substrate conversions within 2 min at 0.02 mol% (93% 1,2-epoxyoctane). This solvent change, however, does not improve substrate conversions with **3** under comparable conditions [24].

The composition of the Mn^{II}/phen catalyst is ambiguous under the reaction conditions as 1:1, 1:2 and 1:3 Mn^{II}:phen complexes are known to form. In glacial acetic acid, 1:1 or 1:3 molar mixtures of $Mn^{II}(CF_3SO_3)_2$ and phen create catalysts that convert ca. 60% of 1-octene at 0.02 mol% Mn^{II}, while a 1:2 mixture provides full 1-octene conversion similar to crystallized **2**. These simple stoichiometric variations of metal and ligand suggest that an active catalyst with two phen ligands. Weakly coordinating anions such as trifluoromethanesulfonate, $CF_3SO_3^-$, are not necessary, as the acetate complex has comparable reactivity under these optimized conditions for **2**.

2.3. Syntheses and characterizations of catalysts

[$Mn^{II}(R,R$-mcp$)(CF_3SO_3)_2$] (**1**) is readily prepared in crystalline form from a 1:1 molar ratio of $Mn^{II}(CF_3SO_3)_2$ and R,R-mcp in anhydrous CH_3CN under N_2, followed by diffusion of Et_2O into the solution. In contrast to **2** and **3**, **1** is hygroscopic and requires anhydrous conditions to obtain X-ray quality crystals. The X-ray structure of **1** reveals a six-coordinate Mn^{II} center with two $CF_3SO_3^-$ bonded in cis sites (Fig. 2). The R,R-mcp ligand adopts a cis-α configuration, since the two terminal pyridine groups are positioned trans to one another. The X-ray structure, solution magnetic susceptibility ($\mu_{eff} = 5.6(3)$ BM) [25], and six-line EPR signal at 77 K with $g \approx 2.0$ are consistent with a high-spin d^5 Mn^{II} complex.

[$Mn^{II}(phen)_2(CF_3SO_3)_2$] (**2**) was synthesized by mixing a 1:2 molar ratio of $Mn^{II}(CF_3SO_3)_2$ and phen in CH_3CN and was crystallized by diffusing Et_2O into the solution in a manner similar to that described for [$Mn^{II}(bpy)_2(CF_3SO_3)_2$] [26]. The structure of **2** shows metrical parameters typical of a high-spin,
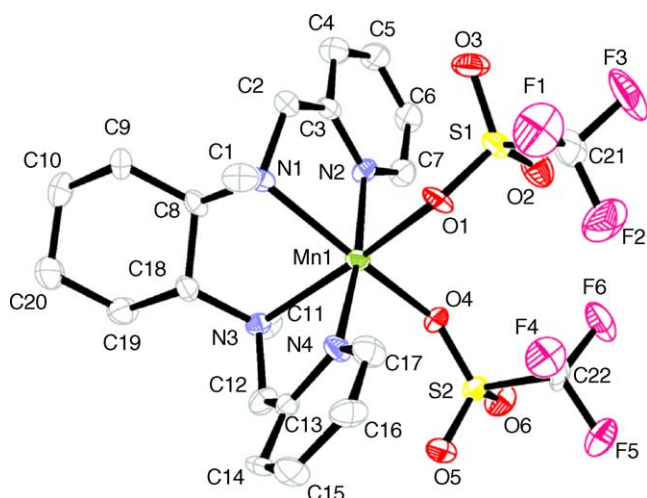
Fig. 2. ORTEP drawing of $[Mn^{II}(R,R\text{-mcp})(CF_3SO_3)_2]$ (**1**) at 50% probability with atom numbering scheme. The hydrogen atoms have been excluded for clarity.

six-coordinate Mn^{II} complex with an average Mn–N distance of 2.23 Å (Fig. 3). The solution susceptibility of $\mu_{eff} = 5.8(3)$ BM [25] and a six-line EPR signal confirm this electronic configuration.

$[Mn^{II}(2\text{-Cl-phen})_2(CF_3SO_3)_2]$ was synthesized in an analogous manner to **2**. The X-ray structure reveals an elongation of the Mn–N bond adjacent to the 2-chloro group (Fig. 4). Relative to the Mn–N distances in **2**, the Mn–N(2,4) distances are lengthened by ~0.1 Å, and the Mn–N(1,3) distances are nearly identical. The solution susceptibility ($\mu_{eff} = 6.1(3)$ BM) [25] and six-line $g \approx 2.0$ EPR signal confirm a high-spin d^5 Mn^{II} complex.

2.4. Proton effect on the epoxidation of 1-octene

The sulfuric acid component in PAA_C inhibits the activity of most Mn^{II} catalysts investigated either through the presence
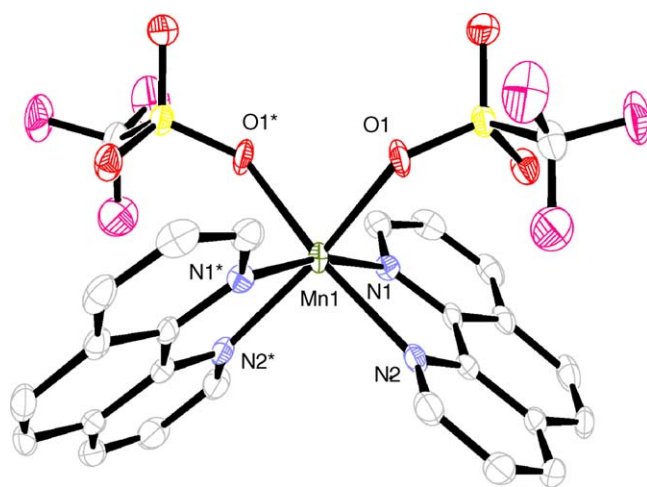

Fig. 4. ORTEP drawing of $[Mn^{II}(2\text{-Cl-phen})_2(CF_3SO_3)_2]$ (**4**) at 50% probability. The Mn–N(1,2,3,4) distances (Å) are 2.24, 2.29, 2.23, and 2.35, respectively. The average Mn–O distance is 2.15 Å. The N(1)–Mn(1)–N(3) and N(2)–Mn(1)–N(4) angles are 173° and 93°, respectively. The hydrogen atoms have been excluded for clarity.

of protons or the anions (HSO_4^{1-} or SO_4^{2-}) [23]. Uncoupling the proton and anion dependence is possible by the addition of $HClO_4$ (70% aqueous solution) to the reaction mixture with PAA_R. As perchlorate is a poorly coordinating anion, the change in epoxidation rates should correlate to the presence of protons. Addition of small quantities of $HClO_4$ attenuate the reactivity of **1** and **2** at 0.02 mol% loading (Figs. 5 and 6). The epoxidation reaction with **2** is much more sensitive to the proton concentration than **1** and is completely inhibited if the proton concentration exceeds 1 mM; a 10-fold increase in the proton concentration is needed for similar inhibition of **1**. The proton sensitivity correlates inversely with the stability constants; the more stable complex **1** tolerates a greater concentration of pro-

Fig. 3. ORTEP drawing of $[Mn^{II}(phen)_2(CF_3SO_3)_2]$ (**2**) at 50% probability. Average Mn–N and Mn–O distances (Å) are 2.23 and 2.18, respectively. The N(1)–Mn(1)–N(1*) and N(2)–Mn(1)–N(2*) angles are 168° and 92°, respectively. The hydrogen atoms have been excluded for clarity.
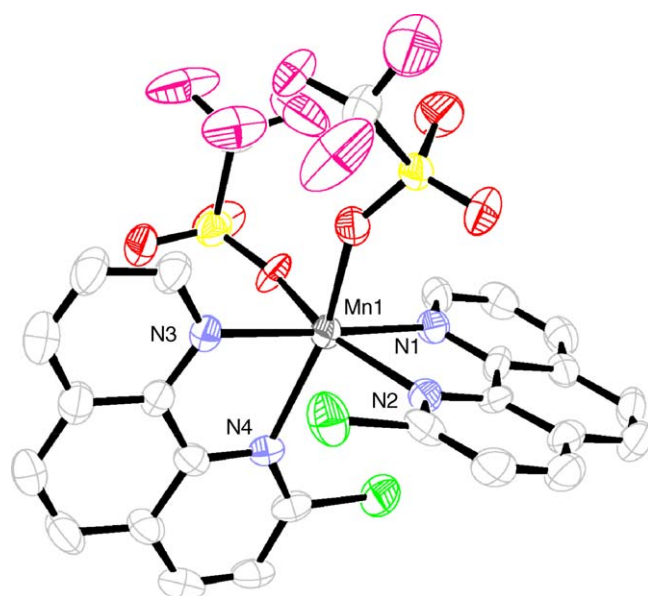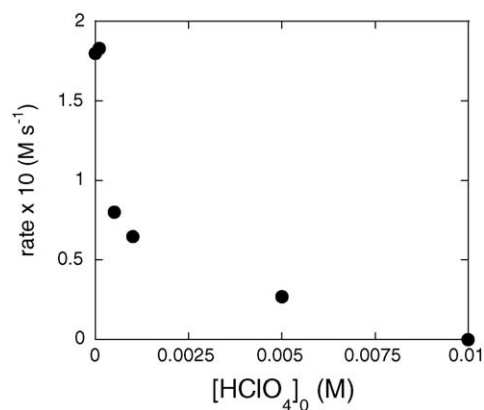

Fig. 5. Initial rate of 1-octene epoxidation relative to the formal perchloric acid concentration $[HClO_4]_0$ with **1** (0.25 M 1-octene, 0.25 M CH_3CO_3H (PAA_R), 0.050 mM **1**, 0.1–10 mM $HClO_4$ in CH_3CN, RT).
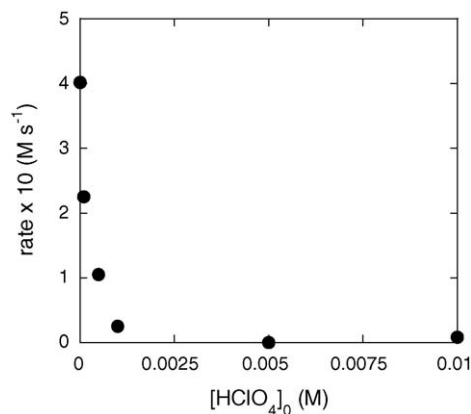
Fig. 6. Initial rate of 1-octene epoxidation relative to the formal perchloric acid concentration $[HClO_4]_0$ with **2** (0.25 M 1-octene, 0.25 M CH_3CO_3H (PAA$_R$), 0.050 mM **2**, 0.1–10 mM $HClO_4$ in CH_3CO_2H, RT).

tons even though the ligand of **1** has much more basic nitrogen atom ligands.

2.5. Nuclearity of the active oxidant and the role of H_2O_2

The epoxidation activity of the monomeric complexes **1** and **2** were compared to their corresponding Mn^{III,IV} bis-μ-oxo dimers [$(R,R$-mcp)$_2$Mn$_2$^{III,IV}(O)$_2$](ClO$_4$)$_3$ (**1d**) and [(phen)$_4$Mn$_2$^{III,IV}(O)$_2$](ClO$_4$)$_3$ (**2d**). Of the two dimers, only **2d** is a competent epoxidation catalyst with PAA$_R$ (0.25 M 1-octene, 0.25 M CH_3CO_3H, 0.025 mM **2d** in CH_3CN at RT, 5 min). Under these reaction conditions, the characteristic Mn^{III,IV}-dimer green color bleaches rapidly with **2d**, but not with **1d**. The initial rates of 1-octene epoxidation by **2** and **2d** are indistinguishable under similar reaction conditions at RT, and in both cases, no induction period to product formation is observed. At lower temperatures (−35 °C) in CH_3CN, a short induction period (ca. 10 s) exists only for **2d**, and the initial rate for **2d** is slightly slower than that observed for **2** (Fig. 7) [27]. The bleaching and induction period at low temperatures is consistent with a reduction of **2d** to monomeric Mn^{II} species, which serve as the catalyst(s) for activating the peracetic acid.
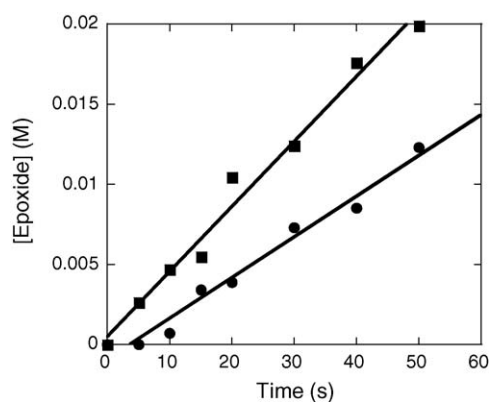

Fig. 7. Initial rates of 1-octene epoxidation with **2** (■) or **2d** (●) at −35 °C (0.25 M 1-octene, 0.25 M CH_3CO_3H (PAA$_R$), 0.25 mM monomer or 0.125 mM dimer in CH_3CN).
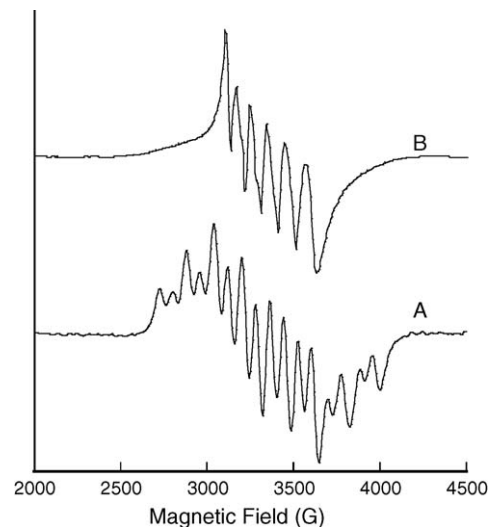

Fig. 8. EPR of **2d** (A) and after the reaction with PAA$_R$ (B) under catalytic conditions (0.25 M 1-octene, 0.25 M CH_3CO_3H (PAA$_R$), 1 mM **2d**, 5 min at 25 °C in CH_3CO_2H).

If **2d** is reduced to monomeric Mn^{II} species, **2** and **2d** should exhibit similar steric and electronic preferences for substrates. Pair-wise competition reactions with *cis*-cyclooctene, 1-octene, and *trans*-ethyl crotonate with **2** and **2d** give a 200:30:1 ratio of epoxides of *cis*-cyclooctene: 1-octene: *trans*-ethyl crotonate, with the relative amounts of epoxide products normalized to the *trans*-ethyl crotonate product [23,28]. For these experiments, 1:1 mixtures of two substrates (1.0 M total olefin) in CH_3CN were mixed with a substoichiometric amount of CH_3CO_3H (0.1 equiv., 0.10 M) to assure limited substrate conversion with each catalyst.

EPR spectroscopy at 77 K is a convenient technique by which to probe Mn speciation under the reaction conditions. The six-line $g \approx 2.0$ EPR signal of **2** indicates a Mn^{II} monomer, which persists throughout the reaction (0.5 M 1-octene, 0.5 M CH_3CO_3H (PAA$_R$), 1.0 mM **2** in CH_3CO_2H, 25 °C), while the sixteen-line $g \approx 2.0$ EPR signal of **2d** is converted rapidly to a signal typical of monomeric Mn^{II} complexes (Fig. 8).

This reduction of **2d** is effected presumably by either the residual H_2O_2 in PAA$_R$ (0.05–0.10 M H_2O_2 under reaction conditions) or peracetic acid itself. Solutions of H_2O_2 in acetic acid rapidly reduce **2d** to monomeric Mn^{II} species in a quantitative manner as assessed by EPR spin-integration (Fig. 9). Perlauric acid, a crystalline peracid that does not contain measurable amounts of H_2O_2, also causes the 16-line signal of **2d** to convert to a Mn^{II} signal, except that spin-integration of the final signal only accounts for ∼5% of the initial Mn content (Fig. 10). UV–vis spectroscopy shows that the green Mn^{III,IV} dimer color does not bleach, but instead is converted to a red color. The weak Mn^{II} EPR signal that results from this perlauric acid reaction with **2d** may result from Mn^{II} impurities in the starting material, as its EPR signal would be obscured by the signal of the dimer. Combined, the data suggest that the residual H_2O_2 and not the peracetic acid is the reductant for Mn^{III,IV} dimers [29].
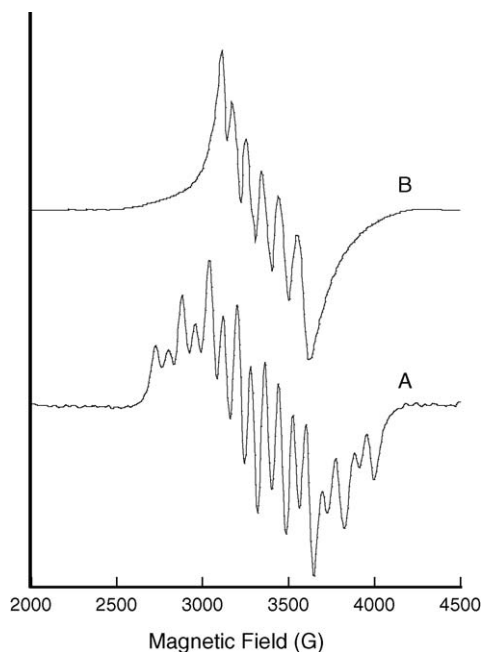
Fig. 9. EPR of **2d** (A) and after addition of 0.25 M H_2O_2 (B) (0.25 M 1-octene, 0.25 M H_2O_2, 1 mM **2d**, 5 min at 25 °C in 5:1 $CH_3CN:CH_3CO_2H$).
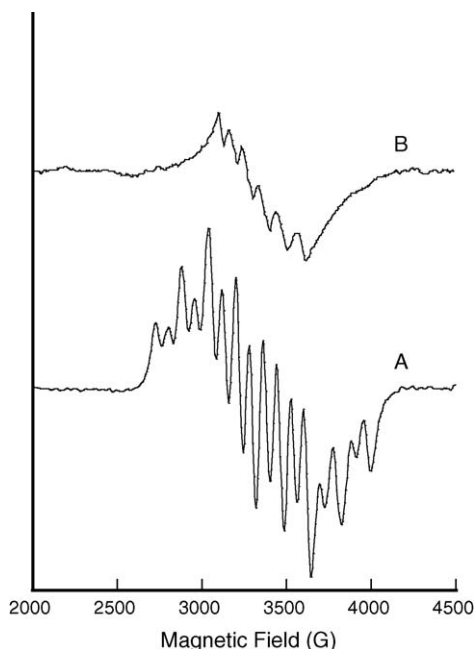

Fig. 10. EPR of **2d** (A) and after addition of 0.25 M perlauric acid (B) (0.25 M 1-octene, 0.25 M perlauric acid, 1 mM **2d**, 5 min at 25 °C in CH_3CN). Spin integration of the two EPR signals shows that spectrum B accounts for ∼5% of the spin present prior to the addition of oxidant.

3. Discussion

3.1. Identification and optimization of terminal olefin epoxidation catalysts

Under appropriate reaction conditions, simple metal salts are known to be effective epoxidation catalysts for terminal olefins, but coordination of more elaborate ligands adds a powerful and

variable dimension to modulating the reactivity of these catalysts [9,30]. In our investigation of mononuclear Mn^{II} catalysts for terminal olefin epoxidation with peracetic acid, ligands were selected and screened to highlight the importance of various attributes for efficient reactivity, which include coordination number, coordinate mode, ligand type and complex stability (Fig. 1). Neutral, tetraamine ligands, which are highly preorganized for metal binding in a non-square planar geometry, produce the most effective mononuclear manganese catalysts. With commercial peracetic acid (PAA_C, pH ∼1) as the oxidant, only 3 of 22 of the manganese complexes are good catalysts for terminal olefin epoxidations: $[Mn^{II}(R,R\text{-mcp})]^{2+}$, $[Mn^{II}(bisp)]^{2+}$ and $[Mn^{II}(Me_3\text{-tacn})]^{2+}$ (Table 1, entries 1, 9, 14) [20,21]. All three have highly preorganized ligands and Mn^{II} coordination geometries that can accommodate at least two exogenous ligands in *cis* binding sites. The limited reactivity of the other Mn^{II} complexes presumably results from rapid Mn^{II} decomplexation affected by the protons of the strongly acidic reaction medium. In larger reactions, $Mn^{II}SO_4$, a white precipitate, appears almost immediately upon mixing PAA_C with many of the catalysts. Of the efficient catalysts under strongly acidic conditions, the reactivity of $[Mn^{II}(R,R\text{-mcp})(CF_3SO_3)_2]$ (**1**) with PAA_C was further optimized given its impressive selectivity and turnover frequency [2].

Peracetic acid solutions synthesized with a strong acid resin (PAA_R [18]) are much less acidic than PAA_C. This ostensibly small change in conditions dramatically alters the performance of many of the Mn^{II} catalysts (Table 1) [22]. Many complexes are competent catalysts with PAA_R at 1 mol% catalyst loading, yet only 6 of 22 are effective at 0.1 mol % catalyst loading with PAA_R: $[Mn^{II}(R,R\text{-mcp})(CF_3SO_3)_2]$ (**1**), $[Mn^{II}(phen)_2(CF_3SO_3)_2]$ (**2**), $[Mn^{II}(bpy)_2(CF_3SO_3)_2]$ (**3**), $[Mn^{II}(5\text{-Cl-phen})_2(CF_3SO_3)_2]$ (**4**), $[Mn^{II}(Me_3tacn)(CF_3SO_3)_2]$, and $[Mn^{II}(bpma)(CF_3SO_3)_2]$. The significant reactivity of **2** and **3** is particularly intriguing given their anemic behavior with the more acidic PAA_C (Table 1). The high turnover frequencies (>50 s^{-1}) and the commercial availability of these oxidatively stable ligands motivated a search for optimized conditions; 2 equiv. of oxidant, 0.5 M substrate, and a 0.02 mol% loading of **1** or **2** in CH_3CN and CH_3CO_2H, respectively, provide reproducible yields and selectivities with simple olefin substrates.

The X-ray structures of **1**, **2**, and **3** [26] show a similar *cis*-N_4 ligation of the six-coordinate Mn^{II} center with $CF_3SO_3^-$ bonded in the two remaining *cis* sites (Figs. 2–4). The energetic preference for such a *cis*-N_4 rather than a *trans*-N_4 coordination is expected for the bis-phen or bis-bpy coordination of **2**–**4**, as a *trans*-N_4 coordination leads to severe interligand steric clashes between aromatic protons positioned *ortho* to the nitrogen atoms. The proclivity of R,R-mcp to adopt a *cis*-N_4 coordination mode in **1** is more subtle, but is consistent with the behavior of other tetradenate ligands that form three, 5-membered rings upon chelation. Yet, a *cis*-N_4 coordination mode is a necessary but not sufficient ligand attribute to assure efficient epoxidation catalysis with PAA; several ligands of Table 1 presumably adopt this metal coordination geometry and their Mn^{II} complexes are poor catalysts. The Mn^{II} complexes of tetradentate

amine ligands that bind in a *trans*-N_4 coordination mode are poor terminal olefin epoxidation catalysts with PAA_R (Me_4-cyclam, Table 1, entries 11). The limited terminal olefin epoxidation of other simple Mn-salen and Mn-porphyrin complexes with *trans* tetradentate ligation is well documented [28,31].

Ligand variations that reduce the thermodynamic, or kinetic stability of the Mn^{II} complex generally attenuate epoxidation activity. In particular, the introduction of sterically demanding groups *ortho* to the pyridyl nitrogen atoms is quite dramatic. Methyl groups in this *ortho*-position introduce not only oxidative instability to the ligand by incorporation of weak benzylic C–H atoms, but also attenuate the pyridyl binding affinity for the Mn^{II} center by elongating the metal–nitrogen bond(s) [32]. A similar elongation is evident in the X-ray structure of $[Mn^{II}(2-Cl-phen)_2(CF_3SO_3)_2]$ (Fig. 4); the Mn^{II}–N distance with an *ortho*-positioned chloride group is elongated by nearly 0.1 Å. A stepwise reduction in activity correlates with the progressive introduction of methyl groups (0, 1, 2) in the series $[Mn^{II}(R,R-mcp)]^{2+}$, $[Mn^{II}(R,R-6-Me-6'-H-mcp)]^{2+}$, and $[Mn^{II}(R,R-6-Me-mcp)]^{2+}$ (Table 1, entries 1, 3, and 4). A similar reduction in reactivity is found for $[Mn^{II}(2-Cl-phen)_2(CF_3SO_3)_2]$ compared to $[Mn^{II}(phen)_2(CF_3SO_3)_2]$ (Table 1, entries 20 and 21), and this effect is not electronic in nature, as the catalytic activity of $[Mn^{II}(5-Cl-phen)_2(CF_3SO_3)_2]$ with a remotely positioned chloride group (Table 1, entry 22) is comparable to $[Mn^{II}(phen)_2(CF_3SO_3)_2]$. We attribute these changes in reactivity primarily to a reduction in the metal stability constant leading to faster metal dissociation under the reaction conditions, though the steric demands of these *ortho*-positioned groups could also adversely influence the binding and potential chelation by the peracid oxidant.

The importance of strong chelation of the metal is evident from the difference in catalytic activity of $[Mn^{II}(R,R-mcp)]^{2+}$ and $[Mn^{II}(mep)]^{2+}$. With PAA_C, the former is an excellent catalyst for 1-octene epoxidation at 1 or 0.1 mol% loading, while the latter is a marginal catalyst at 1 mol% loading and ineffective at 0.1 mol% loading. The *R,R*-mcp and mep ligands are identical except for the degree of organization of the diamine backbone; *R,R*-mcp is constructed from the preorganized *trans*-1,2-cyclohexyl-diamine rather than the more flexible 1,2-ethylene-diamine. The stability constants for metal complexes with the more organized *trans*-1,2-cyclohexyl-diamine backbone are potentially 10^5 larger than the comparable complexes with a 1,2-ethylene-diamine backbone [33]. An analogous correlation between the stability constants and catalytic epoxidation reactivities is found for **2** and **3**. The phen ligand of **2** is more preorganized for metal binding than is the bpy ligand of **3**, leading to a ca. 100-fold larger stability constant for **2** [33]. As binding of bpy or phen to a Mn^{II} center occurs at approximately the same rate, the dissociation of phen must be ca. 100-fold slower [34,35]. Under acidic conditions, the dissociation mechanism of bpy is proposed to involve a stepwise protonation of a bpy ligand, the first step of which requires a rotation and dissociation of one of the pyridine subunits. This pathway is not accessible to phen thereby slowing the dissociation process. This would prolong the catalyst lifetime in an acidic reaction medium.

3.2. Proton sensitivity

Contrary to the beneficial effect of a strong acid component in the catalytic epoxidation of 1-octene by $[(phen)_4Fe_2^{III}\mu-(O)(H_2O)_2]^{4+}$ with peracetic acid [3], the monomeric manganese catalysts of this study all show lesser reactivity with decreasing pH. The epoxidation reactions with **1** and **2** (Figs. 5 and 6) are sensitive to the amount of $HClO_4$ added to the PAA_R. The greater sensitivity of **2** compared to **1** is consistent with the relative stability of these complexes; at low concentrations, the 1:2 metal to phen stoichiometry for **2** will allow significantly more metal release compared to the tetradentate *R,R*-mcp ligand. Yet, the proton sensitivity of the reaction may not only be a result of the decomposition of the catalyst, but also proton dependant steps prior to the rate-limiting step of the reaction.

3.3. Nuclearity of the catalysts

Because $[Mn^{II}(bpy)_2]^{2+}$ and $[Mn^{II}(phen)_2]^{2+}$ can dimerize under oxidative conditions (^tBuOOH in CH_3CN) to form bis-μ-oxo species $[(L)_4Mn_2^{III,IV}(O)_2]^{3+}$ [36,37], we investigated the potential role of these dimers in the epoxidation reactivity with PAA. While the well-characterized $Mn^{III,IV}$ and $Mn^{IV,IV}$ bis-μ-oxo dimers of *R,R*-mcp, phen, and bpy can oxidize substrates by hydrogen atom and hydride abstractions [29,38–44], their documented ability to catalyze epoxidations of olefins is limited [36,45]. Under our reaction conditions with PAA_R, the distinctive EPR or UV–vis features of $[(R,R-mcp)_2Mn_2^{III,IV}(O)_2]^{4+}$ (**1d**) or $[(phen)_4Mn_2^{III,IV}(O)_2]^{3+}$ (**2d**) are not formed starting from the Mn^{II} catalysts. Additionally, **1d** and **2d** are not effective stoichiometric epoxidation agents of terminal olefins in acetic acid or CH_3CN. However, **2d** is a very effective epoxidation catalyst with PAA_R for 1-octene, in fact it is as effective as **2**. In the catalytic reaction with **2d**, the addition of the PAA_R rapidly bleaches the characteristic green color of the dimer, and a short induction period (ca. 10 s) develops at $-35\,°C$ for **2d** (Fig. 7) [46]. Combined, this data suggests a rapid reduction of the dimeric **2d** to monomeric **2** is required for catalysis. Under the reaction conditions, **1d** is a stable dimer, as its color is not bleached and catalysis is not observed.

EPR spectroscopy provides a sensitive probe to the nature of the manganese species in solution. **1** and **2** exhibit the characteristic six-line $g \approx 2.0$ signal of a monomeric Mn^{II} species and these signals persist throughout the epoxidation reaction [47]. Treatment of **2d** with PAA_R rapidly converts its characteristic sixteen-line $g \approx 2.0$ signal to that of a Mn^{II} monomer, consistent with dimer reduction (Fig. 8) [48,49]. By contrast, the EPR spectrum of the catalytically inactive **1d** remains unchanged upon addition of PAA_R [47]. The residual H_2O_2 in PAA_R ($\sim1\%$ by weight of H_2O_2 in PAA_R) is presumably the reductant of **2d**, as shown for $[Mn_2^{IV,IV}(O_3)(Me_3-TACN)_2](PF_6)_2$ [50,51]. Indeed, **2d** is reduced rapidly to monomeric Mn^{II} species by a solution of H_2O_2 in acetic acid (Fig. 9); **1d** is stable to this H_2O_2 solution for times relevant to this catalytic reaction. Perlauric acid ($CH_3(CH_2)_{10}CO_3H$), a pure crystalline peracid, oxidizes **2d** to its red, EPR silent $Mn^{IV,IV}$ dimer (Fig. 10), supporting the

notion that the residual H_2O_2 in the PAA_R rather than peracetic acid serves as the reductant of **2d**. Pair-wise intermolecular substrate competition experiments provides additional evidence that **2** and **2d** operate through similar catalytically active species. Both catalysts yield a 200:30:1 preference for the epoxidation of *cis*-cyclooctene, 1-octene, and ethyl crotonate, repectively. While potentially coincidental, these results combined with the other evidence support a monomeric species as the catalyst.

4. Conclusions

Screening a series of Mn^{II} complexes for terminal olefin epoxidation has allowed the identification of several Mn^{II} catalysts that are capable of significant activity with PAA_C or PAA_R as the oxidant. The composition of the oxidant plays an important role in maintaining the integrity of the Mn^{II} catalyst and reducing high-valent complexes, which are not active catalysts. With PAA_C $[Mn^{II}(R,R\text{-mcp})(CF_3SO_3)_2]$ exhibits excellent activity, epoxidizing terminal olefins with 0.1 mol% catalyst within 5 min. However, higher activity catalysts are possible with PAA_R. Both $[Mn^{II}(phen)_2(CF_3SO_3)_2]$ and $[Mn^{II}(bpy)_2(CF_3SO_3)_2]$ epoxidize 1-octene with 0.1 mol% loading within 15 s with PAA_R. Further optimization revealed that $[Mn^{II}(phen)_2(CF_3SO_3)_2]$ has the highest activity of all catalysts screened, and combines high activity with simple, in situ catalyst preparation. As little as 0.02 mol% loading with PAA_R provides reproducible reactivity with good yields. This demonstrates that high oxidative activity and stability can be achieved without resorting to more extreme strategies such as very electron-deficient [52] or complicated ligands [53].

5. Experimental

5.1. Materials and instrumentation

(R,R)-(+)-cyclohexane-1,2-diamine was resolved as the tartrate salt as previously described [54]. N,N'-bis(2-pyridyl-methyl)-(R,S)-cyclohexane-1,2-diamine (*meso*-hcp) [55], N,N'-bis(2-pyridylmethyl)-$(1R,2R)$-cyclohexane-1,2-diamine (R,R-hcp) [29,38,56], N,N'-dimethyl-N,N'-bis(2-pyridylmethyl)–$(1R,2R)$-cyclohexane-1,2-diamine (R,R-mcp) [29,38,56], N,N'-dimethyl-N,N'-bis(2-(6-methyl-pyridyl)methyl)–$(1R,2R)$-cyclohexane-1,2-diamine (R,R-6-Me-mcp) [57], N,N'-di-methyl-N,N'-bis(2-pyridylmethyl)-ethane-1,2-diamine (mep) [29,38,56], N,N-dimethyl-N',N'-bis(2-pyridylmethyl)-ethane-1,2-diamine (*uns*-mep) [58], N,N,N'-trimethyl-N'-(2-pyridyl-methyl)-ethane-1,2-diamine (tmep) [59], N,N'-bis(3,5-di-*tert*-butylsalicylidene)-(R,R)-cyclohexane-1,2-diamine (H$_2$cdb) [60], *tris*(2-pyridylmethyl)amine (tmpa) [61], 3,7-dimethyl-9-oxo-2,4-di-2-pyridinyl-3,7-diazabicyclo[3.3.1]nonane-1,5-dicarboxylic acid diethyl ester (bisp) [62,63], methyl-bis(2-pyridylmethyl)amine (bpma) [64], and N-(2-pyridylmethyl)-$(1R,2R)$-cyclohexane-1,2-diamine [65] were synthesized as previously described. 1,4,8,11-tetramethyl-1,4,8,11-tetraazacyclotetradecane (Me$_4$cyclam), 1,4,7-trimethyl-1,4,7-triazacyclononane (Me$_3$tacn), 2,2′-bipyridine (bpy), and 2,2′:6′,2″-terpyridine (terpy) were purchased from Aldrich and used

without further purification. $[Mn^{II}(bpy)_2(CF_3SO_3)_2]$ was synthesized as previously described [26]. $[(phen)_4Mn_2^{III,IV}(O)_2]$ $(ClO_4)_3$ was synthesized by the oxidation of $Mn^{II}(OAc)_2$ with $KMnO_4$ in the presences of 1,10-phenanthroline as previously described [66]. $[(phen)_4Mn_2^{IV,IV}\mu\text{-}(O)_2](ClO_4)_4$ was synthesized from $[(phen)MnCl_3]\cdot H_2O$ [42]. $Mn^{II}(CF_3SO_3)_2$ was synthesized from $Mn^{II}(CO_3)$ and triflic acid (Aldrich) [67], and was recrystallized twice from CH_3CN/Et_2O and dried at 150 °C for 5 h under vacuum. 50% H_2O_2 (stabilized) was purchased from Acros Organics. All other chemicals were purchased from Aldrich and used without further purification.

Mass spectroscopy data (High-resolution EI) was collected by the Mass Spectrometry Facility, Department of Pharmaceutical Chemistry, University of California, San Francisco. Gas chromatographic (GC) yields were determined using either a DB-5 capillary column [30 m × 0.53 mm × 5 µm, He 15 psi] or DB-1 capillary column [15 m × 0.25 mm × 0.1 µm, He 10 psi] on a HP 5890 GC. Electronic paramagnetic resonance (EPR) spectra were recorded on a Bruker ER 220D-SRC instrument as frozen solutions at 77 K at X-band frequency in quartz tubes. EPR spectra were fitted with Bruker Simfonia 1.25.

5.1.1. Preparation of 8–10% peracetic acid (PAA$_R$)

Caution: mixtures of H_2O_2 and organic solvents are potentially explosive, all operations should be performed with great care.

The peracetic acid solutions were synthesized following a slightly modified procedure from US patent #2,910,504. Glacial acetic acid (150 g, 2.5 mol) was stirred in a polyethylene bottle, and 50% H_2O_2 (17 g, 0.25 mol) is slowly added at RT. Once homogenous, 5 g of Amberlite IR-120 is added, and the mixture was stirred behind a blast shield at RT for 24 h. The concentration of CH_3CO_3H was determined by integration of the ^{13}C NMR signal of CH_3CO_3H relative to CH_3CO_2H. Analysis by ^{13}C NMR correlates within 5% of the results obtained by standard Ce^{IV}/iodometric titration techniques. The peracetic acid solution was filtered through a 0.1 µm glass microfiber filter and stored in a polyethene bottle at −20 °C.

5.2. Ligand syntheses

5.2.1. N,N′-dipropyl-N,N′-bis(2-pyridylmethyl)-(1R,2R)-cyclohexane-1,2-diamine (R,R-pcp)

N,N'-bis(2-pyridylmethyl)-$(1R,2R)$-cyclohexane-1,2-diamine (1.4 g, 4.78 mmol) was dissolved in 10 mL of triethylamine followed by the addition of 1-iodopropane (1.62 g, 9.6 mmol, 2 equiv.). The solution was refluxed for 7 h, and the excess triethylamine was removed under vacuum. The residue was dissolved in 20 mL of H_2O, and the aqueous phase was extracted with ethyl acetate (3 mL × 75 mL). The organic layers were combined and dried over Na_2SO_4. The solvent was removed under vacuum yielding a light brown oil (1.2 g, 67%). ^1H NMR (CDCl$_3$) δ = 8.4 (2H, s), 7.6 (2H, t), 7.4 (2H, t), 7.0 (2H, t), 3.7 (2H, dd), 2.6 (2H, m), 2.4 (4H, t), 2.1–1.5 (2H, m), 1.4 (4H, t), 1.1 (4H, m), 0.72 (6H, t). ^{13}C NMR (CDCl$_3$)

$\delta = 161.5$, 147.4, 135.2, 122.4, 120.6, 60.5, 55.9, 52.0, 28.4, 25.3, 21.34, 11.1. HRMS $[M^+]$, calculated $m/z = 380.2940$, found $m/z = 380.2942$.

5.2.2. N,N,N′-trimethyl-N′-(2-pyridylmethyl)-(R,R)-cyclohexane-1,2-diamine (R,R-tmcp)

N-(2-pyridylmethyl)–(1R,2R)-cyclohexane-1,2-diamine [65] (0.114 g, 0.56 mmol) was dissolved in 5 mL of H_2O. 37% formaldehyde in H_2O (0.56 g, 6.9 mmol, 12 equiv.) was added, followed by 97% formic acid (0.271 g, 5.6 mmol, 10 equiv.). The solution was heated to reflux for 10 h, cooled, and diluted with 5 mL of 6 M NaOH after cooling. The aqueous phase was extracted with CH_2Cl_2 (2 mL × 20 mL). The organic layers were combined and dried over Na_2SO_4. The solvent was removed under vacuum yielding a light brown oil (0.114 g, 83%). ^1H NMR ($CDCl_3$) $\delta = 8.4$ (1H, s), 7.6 (2H, m), 7.1 (1H, t), 3.8 (2H, q), 2.5 (2H, s), 2.29 (6H, s), 2.26 (3H, s), 2.0–1.0 (8H, m). ^{13}C NMR ($CDCl_3$) $\delta = 160.1$, 147.8, 135.6, 122.4, 120.9, 63.2, 62.7, 60.2, 39.3, 35.4, 24.9, 24.8, 24.5, 23.0. HRMS $[M^+]$, calculated $m/z = 247.2048$, found $m/z = 247.2053$.

5.2.3. N,N′-dimethyl-N-(2-pyridylmethyl)-N′-(6-methyl-2-pyridylmethyl)-(1R,2R)-cyclohexane-1,2-diamine (R,R-6-H-6′-Me-mcp)

N-(2-pyridylmethyl)-(1R,2R)-cyclohexane-1,2-diamine [65] (0.3 g, 1.47 mmol) was dissolved in 10 mL of EtOH. A 6-methyl-2-pyridinecarboxaldehyde (0.178 g, 1.47 mmol) was added, and the solution was refluxed for 10 min. The solution was cooled, and solid $NaBH_4$ (0.280 g, 7 mmol) was added slowly. The solution was heated to reflux for 5 h, cooled, and the EtOH was removed under vacuum. The residue was dissolved in 20 mL of H_2O, and extracted with CH_2Cl_2 (2 mL × 20 mL). The organic layers were combined and the solvent was removed under vacuum yielding a light brown oil.

This crude oil was subjected to an Eschweiler–Clarke methylation without further purification. The oil was dissolved in 5 mL H_2O. Thirty-seven percentage formaldehyde in H_2O (1.11 g, 13 mmol) was added, followed by 97% formic acid (0.611 g, 13 mmol). The solution was heated to reflux for 10 h, cooled, and diluted with 5 mL of 6 M NaOH. The aqueous phase was extracted with CH_2Cl_2 (2 mL × 20 mL). The organic layers were combined and dried with Na_2SO_4. The solvent was removed under vacuum yielding a light brown oil (0.35 g, 72% for two steps). ^1H NMR ($CDCl_3$) $\delta = 8.5$ (1H, d), 7.8–7.4 (3H, m), 7.2–6.9 (3H, m), 3.8 (4H, m), 2.70–2.51 (2H, m), 2.53 (3H, s), 2.49 (3H, s), 2.38 (3H, s), 2.4–1.0 (8H, m). ^{13}C NMR ($CDCl_3$) $\delta = 148.5$, 136.5, 136.4, 136.2, 122.9, 122.8, 121.6, 121.5, 121.2, 120.9, 119.5, 64.6, 64.3, 60.3, 60.2, 36.5, 31.6, 25.9, 25.7, 25.5, 25.4. HRMS $[M^+]$, calculated $m/z = 338.2470$, found $m/z = 338.2458$.

5.2.4. N-(3,5-di-t-butyl-butylsalicylidene)-N′-(2-pyridylmethyl)-(R,R)-cyclohexane-1,2-diamine (R,R-H₁pcdb)

N-(2-pyridylmethyl)-(R,R)-cyclohexane-1,2-diamine [65] (0.171 g, 0.8 mmol) was dissolved in 20 mL of i-PrOH, and 3,5-di-t-butyl-6-hydroxy-benzaldehyde (0.196 g, 0.8 mmol)

was added. The solution was refluxed for 5 min, and the solvent was removed under vacuum. The residue was purified by column chromatography on basic alumina eluting with a 100% hexane to 100% Et_2O gradient until the residual aldehyde had eluted, followed by 9:1 Et_2O:acetone to remove the desired product. The appropriate fractions were combined, and the solvent was removed under vacuum yielding a bright yellow wax (0.260 g, 77%). ^1H NMR ($CDCl_3$) $\delta = 8.50$ (1H, d), 8.44 (1H, s), 7.57 (1H, t), 7.39 (1H, s), 7.26 (1H, s), 7.23 (1H, d), 7.09 (1H, m), 3.93 (2H, q), 3.05 (1H, m), 2.63 (2H, m), 2.18 (2H, m), 1.7–1.1 (23H, m). ^{13}C NMR ($CDCl_3$) $\delta = 165.1$, 148.8, 135.9, 126.4, 126.3, 125.6, 121.7, 121.4, 117.5, 73.4, 59.7, 51.5, 34.6, 33.7, 33.5, 31.0, 30.99, 30.90, 30.0, 29.0, 28.8, 28.3, 24.2. HRMS $[M^+]$, calculated $m/z = 421.3093$, found $m/z = 421.3088$.

5.3. Reactivity

5.3.1. Epoxidation reactivity with 1-octene

A 5 mM solution of **1** was prepared by dissolving R,R-mcp (3.26 mg, 10.1 mmol) in a 5 mM solution of $Mn^{II}(CF_3SO_3)_2$ in CH_3CN (2.025 mL, 10.1 mmol $Mn^{II}(CF_3SO_3)_2$). The 5 mM solution of **1** (0.1 mL) was placed in a 10 mm × 150 mm test tube along with 1-octene (5.5 mg, 0.05 mmol) and n-nonane (1 μL). Two equivalent of peracetic acid (0.1 mmol) were rapidly syringed into the solution. The mixture was shaken until homogenous, quenched after 5 min by diluting with Et_2O, and filtered through a basic alumina plug. GC analysis of the solution provides the substrate conversion and product yield relative to the internal standard integration. The epoxide product was identified by comparison to the GC retention time of an authentic sample.

5.3.2. Standard condition for kinetic studies

To a solution of alkene (0.5 M in CH_3CO_2H, 100 μL) and n-nonane (1 μL) in a 150 mm × 10 mm test tube at 25 °C $[Mn^{II}(L)(CF_3SO_3)_2]$ was added (5 mM in CH_3CN, 2 μL, 0.02 mol%), followed by gentle mixing. Peracetic acid (100 μL 1.0 M in CH_3CO_2H (PAA$_R$), 70 μL 9.5% PAA and 30 μL HOAc) was added rapidly with mixing. The reaction was quenched at the appropriate time by addition of Et_3N, diluted with Et_2O, filtered through a basic alumina plug, and analyzed by GC. For rates measured at sub-ambient temperatures, solutions of olefin and oxidant were prepared in CH_3CN.

5.4. Synthesis and crystallization of Mn^{II} complexes

5.4.1. Synthesis of [Mn^{II}(R,R-mcp)(CF₃SO₃)₂]

Under an N_2 atmosphere, N,N′-dimethyl-N,N′-bis(2-pyridylmethyl)-(1R,2R)-(+)-cyclohexane-1,2-diamine (R,R-mcp, 322 mg, 1 mmol) was dissolved in 3 mL of CH_3CN along with 353 mg of $Mn^{II}(CF_3SO_3)_2$ (0.99 mmol). Once homogenous, Et_2O was carefully layered on the solution to induce crystallization over 12 h. The crystals were isolated by vacuum filtration and washed with cold Et_2O to yield 0.480 mg (71%) of a brown, hydroscopic crystalline powder. X-ray quality crystals were grown from a CH_3CN solution with Et_2O diffusion. Anal. Calcd. for $MnS_2F_6O_6N_4C_{22}H_{28}$: C 39.00; H 4.17; N 8.27.

Found: C 38.52; H 3.95; N 7.99. μ_{eff} = 5.6 BM (22 °C, CH$_3$CN) [25].

5.4.2. Synthesis of [Mn^{II}(1,10-phenanthroline)(CF$_3$SO$_3$)$_2$]

Mn^{II}(CF$_3$SO$_3$)$_2$ (0.506 g, 1.4 mmol) and 1,10-phenanthroline (0.498 g, 2.8 mmol) were dissolved in 25 mL of dry CH$_3$CN to produce a bright yellow solution. Once a homogenous solution was obtained with stirring (ca. 10 min), 30 mL of Et$_2$O was layered carefully on the solution to induce crystallization over 12 h. The crystals were isolated by vacuum filtration, washed with cold Et$_2$O to yield 0.428 mg (42%) of translucent yellow crystals. Anal. Calcd. for MnS$_2$F$_6$O$_6$N$_4$C$_{26}$H$_{16}$: C 43.77; H 2.26; N 7.85. Found: C 43.61; H 2.31; N 7.88. μ_{eff} = 5.8 BM (22 °C, CH$_3$CN) [25].

5.4.3. Synthesis of [Mn^{II}(2-chloro-1,10-phenanthroline)$_2$(CF$_3$SO$_3$)$_2$]·2H$_2$O

Mn^{II}(CF$_3$SO$_3$)$_2$ (0.124 g, 0.35 mmol) and 2-chloro-1,10-phenanthroline (0.150 g, 0.79 mmol) were dissolved in 5 mL of dry CH$_3$CN to produce a faint yellow solution. Once homogenous, 5 mL of Et$_2$O was carefully layered on the solution to induce crystallization over 12 h. The crystals were isolated by vacuum filtration, washed with cold Et$_2$O to yield 0.428 mg (42%) of translucent yellow crystals. Anal. Calcd. for MnS$_2$F$_6$Cl$_2$O$_8$N$_4$C$_{26}$H$_{16}$: C 39.71; H 2.30; N 7.12. Found: C 39.63; H 1.90; N 7.18. μ_{eff} = 6.1 BM (22 °C CH$_3$CN) [25].

5.5. EPR

5.5.1. EPR analysis of the reaction of 2d with oxidants

A solution containing [(phen)$_4$Mn$_2$^{III,IV}(O)$_2$](ClO$_4$)$_3$ (**2d**) and 1-octene (2 mM 2d, 0.5 M 1-octene in CH$_3$CN, 250 μL) was placed in a 13 mm × 100 mm test tube, followed by the rapid addition of CH$_3$CO$_3$H (0.25 M CH$_3$CO$_3$H (PAA$_R$) in CH$_3$CN, 250 μL). Once homogeneous, the solution was transferred to an EPR tube and frozen in lN$_2$.

5.6. X-ray crystallographic analysis

X-ray diffraction quality crystals were mounted under a cooled N$_2$ stream on a quartz fiber with Paratone *N* hydrocarbon oil on a Bruker–Siemens SMART [68] CCD with graphite monochromated Mo Kα radiation or at the Advanced Light Source at the Lawence Berkeley Laboratories. Cell constants and an orientation matrix for data collection were obtained from a least-squares refinement using more than 1000 reflections in the range $4° < 2\theta < 50°$. The space groups were determined based on the systematic absences, packing considerations, a statistical analysis of intensity distribution, and the successful solution and refinement of the structure. Data were integrated by the program SAINT [69], and equivalent non-Friedel reflections were merged. No decay correction was applied. Data were analyzed for agreement and possible absorption using SADABS [70], and a semi-empirical absorption correction was applied in all three cases. The data were corrected for Lorentz and polarization effects. The structures were solved by direct methods and expanded using Fourier techniques, and the hydrogen atoms

were positioned. All calculations were performed using the CrystalStructure crystallographic software package with Shelx as the refinement package [71–73].

Appendix A. Supplementary data

Supplementary data associated with this article can be found, in the online version, at doi:10.1016/j.molcata.2006.01.042.

References

[1] R.A. Sheldon, J.K. Kochi, Metal Catalyzed Oxidations of Organic Compounds, Academic Press, New York, 1981.
[2] A. Murphy, G. Dubois, T.D.P. Stack, J. Am. Chem. Soc. 125 (2003) 5250–5251.
[3] G. Dubois, A. Murphy, T.D.P. Stack, Org. Lett. 5 (2003) 2469–2472.
[4] M.C. White, A.G. Doyle, E.N. Jacobsen, J. Am. Chem. Soc. 123 (2001) 7194–7195.
[5] C. Coperet, H. Adolfsson, K.B. Sharpless, Chem. Commun. (1997) 1565–1566.
[6] K. Sato, M. Aoki, M. Ogawa, T. Hashimoto, R. Noyori, J. Org. Chem. 61 (1996) 8310–8311.
[7] D.E. De Vos, B.F. Sels, M. Reynaers, Y.V.S. Rao, P.A. Jacobs, Tetrahedron Lett. 39 (1998) 3221–3224.
[8] X. Zuwei, Z. Ning, S. Yu, L. Kunlan, Science 292 (2001) 1139–1141.
[9] B.S. Lane, K. Burgess, Chem. Rev. 103 (2003) 2457–2473.
[10] S.E. Schaus, B.D. Brandes, J.F. Larrow, M. Tokunaga, K.B. Hansen, A.E. Gould, M.E. Furrow, E.N. Jacobsen, J. Am. Chem. Soc. 20 (2002) 1307–1315.
[11] D. Swern (Ed.), Organic Peroxides, vol. 1, J Wiley & Sons, Inc., 1970, p. 654.
[12] S. Banfi, F. Montanari, S. Quici, S.V. Barkanova, O.L. Kaliya, V.N. Kopranenkov, E.A. Lukyanets, Tetrahedron Lett. 36 (1995) 2317–2320.
[13] K. Machii, Y. Watanabe, I. Morishima, J. Am. Chem. Soc. 117 (1995) 6691.
[14] J.T. Groves, Y. Watanabe, Inorg. Chem. 25 (1986) 4808–4810.
[15] D.E. de Vos, T. Bein, J. Organomet. Chem. 520 (1996) 195–200.
[16] D.E. De Vos, B.F. Sels, M. Reynaers, Y.V.S. Rao, P.A. Jacobs, Tetrahedron Lett. 39 (1998) 3221–3224.
[17] A. Berkessel, C.A. Sklorz, Tetrahedron Lett. 40 (1999) 7965–7968.
[18] A.T. Hawkinson, W.R. Schmitz, US 2,910,504, E.I. du Pont de Nemours & Co., 1959.
[19] A 10% CH$_3$CO$_3$H solution with a pH of ∼4 is generated by stirring 50% H$_2$O$_2$ with 10 equiv. of CH$_3$CO$_2$H and Amberlite IR-120 resin. These solutions typically have <1% residual H$_2$O$_2$. See Ref. [18].
[20] Complexes with acetate anions have been found to have identical reactivity to the triflate complexes.
[21] Catalysis stops within 15 min for most catalysts.
[22] The chiral ligands tested under these conditions all show enantiomeric excesses <15%.
[23] A. Murphy, A. Pace, T.D.P. Stack, Org. Lett. 6 (2004) 3119–3122.
[24] The rate of epoxidation of 1-octene with [Mn^{II}(bpy)$_2$(CF$_3$SO$_2$)$_2$] is twofold slower than the phen complex under identical conditions.
[25] S.K. Sur, J. Magn. Reson. 82 (1989) 169–173.
[26] J.A. Smith, J.R. Galan-Mascaros, R. Clerac, J.S. Sun, O.Y. Xiang, K.R. Dunbar, Polyhedron 20 (2001) 1727–1734.

[27] The rate of epoxidation of 1-octene with [Mn(phen)$_2$(CF$_3$SO$_3$)$_2$] was found to be similar in CH$_3$CN and CH$_3$CO$_2$H under ambient conditions.

[28] K. Srinivasan, P. Michaud, J.K. Kochi, J. Am. Chem. Soc. 108 (1986) 2309–2320.

[29] J. Glerup, P.A. Goodson, A. Hazell, R. Hazell, D.J. Hodgson, C.J. McKenzie, K. Michelsen, U. Rychlewska, H. Toftlund, Inorg. Chem. 33 (1994) 4105–4111.

[30] Q.H. Xia, H.Q. Ge, C.P. Ye, Z.M. Liu, K.X. Su, Chem. Rev. 105 (2005) 1603–1662.

[31] J.P. Collman, J.I. Brauman, B. Meunier, S.A. Raybuck, T. Kodadek, Proc. Natl. Acad. Sci. USA 81 (1984) 3245–3248.

[32] K. Chen, M. Costas, L. Que, J. Chem. Soc., Dalton Trans. (2002) 672–679.

[33] A.E. Martell, R.M. Smith (Eds.), Critical Stability Constants, Plenum, New York, 1976.

[34] R.H. Holyer, C.D. Hubbard, S.F.A. Kettle, R.G. Wilkins, Inorg. Chem. 4 (1965) 929.

[35] D.N. Hague, S.R. Martin, J. Chem. Soc., Dalton Trans. (1974) 254–258.

[36] S. Ménage, M.N. Collomb-Dunand-Sauthier, C. Lambeaux, M. Fontecave, J. Chem. Soc., Chem. Commun. (1994) 1885–1886.

[37] The trimeric species [Mn$_3$O$_4$(bpy)$_4$(H$_2$O)$_2$](ClO$_4$)$_4$ has been shown to have significant epoxidation reactivty with oxone as the oxidant:. J. Wessel, R.H.J. Crabtree, Mol. Catal. A: Chem. 113 (1996) 13;
J.E. Sarneski, D. Michos, H.H. Thorp, M. Didiuk, T. Poon, J. Blewitt, G.W. Brudvig, R.H. Crabtree, Tetrahedron Lett. 32 (1991) 1153.

[38] P.A. Goodson, J. Glerup, D.J. Hodgson, K. Michelsen, H. Weihe, Inorg. Chem. (1991) 4909–4914.

[39] S.R. Cooper, M. Calvin, J. Am. Chem. Soc. 99 (1977) 6623–6630.

[40] M. Stebler, A. Ludi, H.B. Burgi, Inorg. Chem. 25 (1986) 4743–4750.

[41] H.A. Goodwin, R.N. Sylva, Aust. J. Chem. 18 (1965) 1743–1749.

[42] H.A. Goodwin, R.N. Sylva, Aust. J. Chem. 20 (1967) 629–637.

[43] R. Manchanda, H.H. Thorp, G.W. Brudvig, R.H. Crabtree, Inorg. Chem. 31 (1992) 4040–4041.

[44] M.-N.C. Dunand-Sauthier, A. Deronzier, A. Piron, X. Pradon, S. Ménage, J. Am. Chem. Soc. 120 (1998) 5373–5380.

[45] A.S. Larsen, K. Wang, M.A. Lockwood, G.L. Rice, T.J. Won, S. Lovell, M. Sadilek, F. Turecek, J.M. Mayer, J. Am. Chem. Soc. 28 (2002) 10112–10123.

[46] The, Mn^{IV,IV} dimer shows similar kinetic behavior to the Mn^{III,IV} dimer.

[47] See Supporting Information.

[48] K.-O. Schaefer, R. Bittl, W. Zweygart, F. Lendzian, G. Haselhorst, T. Weyhermueller, K. Wieghardt, W. Lubitz, J. Am. Chem. Soc. 120 (1998) 13104–13120.

[49] K.O. Schaefer, R. Bittl, F. Lendzian, V. Barynin, T. Weyhermueller, K. Wieghardt, W. Lubitz, J. Phys. Chem. B 107 (2003) 1242–1250.

[50] B.C. Gilbert, J.R. Lindsay Smith, A. Mairata i Payeras, J. Oakes, R. Pons i Prats, J. Mol. Catal., A Chem. 219 (2004) 265–272.

[51] B.C. Gilbert, J.R.L. Smith, A. Mairata i Payeras, J. Oakes, Org. Biomol. Chem. 2 (2004) 1176–1180.

[52] S. Banfi, M. Cavazzini, F. Coppa, S.V. Barkanova, O.L. Kaliya, J. Chem. Soc., Perkin Trans. 2 (1997) 1577–1583.

[53] M.L. Merlau, M.D.P. Mejia, S.T. Nguyen, J.T. Hupp, Angew. Chem., Int. Ed. 40 (2001) 4239–4242.

[54] J.F. Larrow, E.N. Jacobsen, Y. Gao, Y.P. Hong, X.Y. Nie, C.M. Zepp, J. Org. Chem. 59 (1994) 1939–1942.

[55] R.R. Fenton, R.S. Vagg, P. Jones, P.A. Williams, Inorg. Chim. Acta 128 (1987) 219–229.

[56] P.A. Goodson, J. Glerup, D.J. Hodgson, K. Michelsen, U. Rychlewska, Inorg. Chem. (1994) 359–366.

[57] D.-H. Jo, Y.-M. Chiou, L. Que Jr., Inorg. Chem. 40 (2001) 3181–3190.

[58] M. Weitzer, M. Schatz, F. Hampel, F.W. Heinemann, S. Schindler, J. Chem. Soc., Dalton Trans. 5 (2002) 686–694.

[59] B.A. Markies, P. Wijkens, J. Boersma, H. Kooijman, N. Veldman, A.L. Spek, G. van Koten, Organometallics 13 (1994) 3244–3258.

[60] E.N. Jacobsen, W. Zhang, A.R. Muci, J.R. Ecker, L. Deng, J. Am. Chem. Soc. 113 (1991) 7063–7064.

[61] J.B. Mandel, C. Maricondi, B.E. Douglas, Inorg. Chem. 27 (1988) 2990–2996.

[62] T. Siener, A. Cambareri, U. Kuhl, W. Englberger, M. Haurand, B. Koegel, U. Holzgrabe, J. Med. Chem. 43 (2000) 3746–3751.

[63] P. Comba, B. Kanellakopulos, C. Katsichtis, A. Lienke, H. Pritzkow, F. Rominger, J. Chem. Soc., Dalton Trans. (1998) 3997–4002.

[64] B. De Bruin, J.A.W. Verhagen, C.H.J. Schouten, A.W. Gal, D. Feichtinger, D.A. Plattner, Chem. Eur. J. 7 (2001) 416–422.

[65] P.D. Newman, P.A. Williams, F.S. Stephens, R.S. Vagg, Inorg. Chim. Acta 183 (1991) 145–155.

[66] R. Manchanda, G.W. Brudvig, S. de Gala, R.H. Crabtree, Inorg. Chem. 33 (1994) 5157–5160.

[67] Y. Inada, Y. Nakano, M. Inamo, M. Nomura, S. Funahashi, Inorg. Chem. (2000) 4793–4801.

[68] SMART: Area-Detector Software Package, Siemens Industrial Automation Inc., Madison, WI, 1995.

[69] SAINT: SAX Area-Detector Integration Program 4.024, Siemens Industrial Automation Inc., Madison, WI, 1995.

[70] SADABS: Siemens Area Detector Absorption Correction Program 2.05, Bruker AXS Inc., Madison, WI, 1998.

[71] D.T. Watkin, J.R. Carruthers, Crystals, Chemical Crystallography Laboratory, Oxford University, Oxford, 1984.

[72] G.M. Sheldrick, SHELX-97, University of Gottingen, Germany, 1997.

[73] Rigaku, Rigaku/MSC CrystalStructure 3.5.1: Crystal Structure Analysis Package (2003), The Woodlands, TX.